RSC Advances

This is an *Accepted Manuscript*, which has been through the Royal Society of Chemistry peer review process and has been accepted for publication.

Accepted Manuscripts are published online shortly after acceptance, before technical editing, formatting and proof reading. Using this free service, authors can make their results available to the community, in citable form, before we publish the edited article. This *Accepted Manuscript* will be replaced by the edited, formatted and paginated article as soon as this is available.

You can find more information about *Accepted Manuscripts* in the **Information for Authors**.

ROYAL SOCIETY
OF **CHEMISTRY**

www.rsc.org/advances

RSC Advances

Largely enhanced fracture toughness of an immiscible polyamide 6/acrylonitrile-butadiene-styrene blend achieved by adding chemically modified graphene oxide

Wenbin Huang, Tingting Zhang, Jinghui Yang*, Nan Zhang, Ting Huang, Yong Wang*

Key Laboratory of Advanced Technologies of Materials (Ministry of Education), School of Materials Science and Engineering, Southwest Jiaotong Universtiy, Erhuan Road, North I, No 111, Chengdu, Sichuan 610031, China

Abstract: In this work, chemically modified graphene oxide was successfully prepared by emulsion polymerization of styrene, leading to grafting polystyrene (PS) onto graphene oxide (GO). Different contents of polystyrene grafted graphene oxide (PS-GO) were incorporated into immiscible polyamide 6/acrylonitrile-butadiene-styrene (PA6/ABS) blend and it was expected that PS-GO could tune the morphology and improve mechanical property. The mechanical testing showed a great improvement on ductility of polymer blends, in which the elongation at break increased by nearly 400% and the impact strength increased by nearly 200% with only 0.5 wt% PS-GO. The underlying mechanism for toughening was carefully discussed via investigations on effects of PS-GO on morphology, chain mobility as well as interfacial interaction. The morphology changes of the blend with PS-GO show slight increase of continuity of ABS. The fracture morphologies showed that the addition of PS-GO induced enhanced interfacial adhesion, exhibiting finer fracture morphology. DMA results verified the enhanced interfacial interaction between ABS and PA6 with the addition of PS-GO. Furthermore, the results demonstrated the interface localization of PS-GO in PA6/ABS. Combined with these observations, it was suggested that the PS-GO located at interface of immiscible blends PA6/ABS and enhanced the interfacial adhesion via the dual interactions with two components, in which one was the electronic stacking interaction between grafted

*Corresponding author: Tel: +86 28 87602714(J H.Yang), +86 28 87603042 (Y. Wang) E-mail addresses: yangjinghui_84@163.com(J H. Yang), yongwang1976@163.com (Y. Wang)

PS on PS-GO and ABS while the other one was the interaction between polar groups on PS-GO and PA6, finally resulting in a great improvement on ductility.

Keywords: chemically modified graphene oxide, interfacial adhesion, toughening

1. Introduction

Polymer blending is an effective and economical way to develop new materials with synergistic properties, and has attracted a great number of scientists and researchers [1]. By varying the composition of polymers or tailoring processing methods, a variety of morphologies and its resultant properties can be achieved. However, the unfavorable enthalpy of mixing two polymers often leads to macro phase separation of polymer blends, which further results in weak interfacial adhesion with few chain entanglements. The resultant mechanical properties, especially for toughness or ductility, are deteriorated [2, 3]. Hence, improving the interface adhesion is important to achieve the exceptional properties via blending two polymers. The classical approach to tailor the interfacial adhesion is to incorporate copolymers which act as emulsifiers/surfactants to lower the interfacial tension, resulting in an interfacial enhancement or compatibilization of polymer blends [4, 5].

Recently, the addition of nanofillers to an immiscible blend has become a new pathway to tailor the morphology of polymer blends and has also aroused great interests [6, 7, 8]. Firstly, the selective adsorption of polymer chains on nanofillers can rebuild the thermodynamic states of polymer blends, leading to a variety of morphologies; secondly, the localization of nanofillers at interface can retard the coalescence of phase domain to further stabilize the phase structures. Besides these effects, the nanofillers impart attractive properties, such as extra-high modulus and strength, excellent conductivity, and optical and magnetic functions. Among these nanofillers, graphene and its derivatives, as new types of two-dimensional fillers, have attracted a great deal of interest. They are widely applied for the strengthening and

toughening the polymer materials because of their intrinsic excellent properties [9, 10] and enhanced interfacial adhesion which is contributed by the large aspect ratio and wrinkles of "soft" graphene [11]. For example, Rafiee et al firstly reported considerably enhanced fracture toughness of graphene filled epoxy composites. The toughness of graphene filled epoxy showed an increase with only 0.125 wt% graphene. The toughening mechanism was ascribed to the effective crack deflections induced by enhanced specific surface areas and two-dimensional geometry of graphenes [12]. Specially, graphene oxide (GO), which has been extensively investigated as promising precursors for the mass production of graphene, exhibits a unique type of building block with hydrophilic oxidative debris on the edge and hydrophobic domains on the basal plane [11, 13, 14]. Therefore, GO exhibits amphiphilic feature, and is applied in polymer blended materials as surfactants or emulsifiers. Feng et al firstly incorporated GO into an immiscible PA6/polyphenylene oxide (PPO) blends, and compatibilization of blends can be realized due to the electronic stacking interaction between GO sheets and PPO as well as the hydrogen bonding between oxidized groups and PA6[15]. In a similar way, Feng et al demonstrated that GO covalently functionalized with polypropylene (PP) chains was potent compatibilizers for PP/PPO blends, because the PP chains grafted on GO could strengthen the interfacial entanglement between GO and nonpolar PP [16]. Finer morphologies and higher ductility of PS/ polymethyl methacrylate (PMMA) was induced by the GO sheets grafted with the P (St-co-MMA) copolymer [17]. With the development of chemical functionalization, the GO with high reactivity can be effectively decorated by a variety of chemical groups, and followed by reduction to obtain various chemically grafted graphene [18, 19, 20]. Based on the emergency of GO decorated by various functional groups, graphene and its derivatives based polymer nanocomposites have been extensively investigated. [21, 22, 23.]

Immiscible blends of PA6 and acrylonitrile-butadiene-styrene (ABS) are of commercial significance in industrial products. However, inherent immiscibility between ABS and PA6 limits their application in developing new materials, especially interfacial adhesion is still a weak point. As we mentioned above, graphene and its derivatives are good candidates for improving interactions between two polymers due to the "amphiphilic" effects originated from possible interaction between chemically modified graphene and polymer pairs. In this way, polystyrene (PS) grafted graphene oxide is chemically designed to strengthen interfacial adhesion of the immiscible blends PA6/ABS. It is expected that in the blend composites, PS chains on the edge is proposed to strengthen the interaction between PS-GO and ABS; and PA6 could form hydrogen bonding with oxidized groups on the PS-GO. It is demonstrated that upon only 0.5 wt% PS-GO was incorporated into PA6/ABS, the elongation at break as well as impact strength shows great improvement. The underlying toughening mechanisms are carefully discussed in a viewpoint of interfacial adhesion induced by chemically modified reduced graphene oxide.

2. Experimental

2.1 Materials

All the materials used in this study are commercially available. PA6 (TP4208) with a melt flow rate (MFR) of 35.5 g/10 min (225 °C/2.16 kg) was obtained from Zig Sheng Industrial co., Ltd., PR China. ABS (PA757) with MFR of 1.8 g/10 min (200 °C/5 kg) was supplied by CHIMEI CORPORATION. Graphite powder with an average particle size of 10-20 μm and a purity of >95% were purchased from Qingdao Heilong Graphite Co., Ltd. Graphene oxide (GO) were prepared from natural graphite powder by oxidation with $KMnO_4$ in concentrated H_2SO_4 according to modified Hummers method [24]. All other chemicals were obtained as analytical grade products and used without further purification.

2.2 Fabrication

2.2.1 Fabrication of PS-GO

About 500 mg GO were dispersed in 200 ml deionized water in a 500 ml round-bottom flask,0.5 g SDS and 30 ml styrene monomer were added into the flask, followed by 30 min of ultrasonic irradiation. Afterwards, 0.5 g $K_2S_2O_8$ was added into the mixture and the reaction mixture was refluxed at 80 °C for 5 h under a nitrogen atmosphere for polymerization. Then, 10 ml hydrazine hydrate was added into the chemically modified graphene oxide dispersion and the reaction mixture was again refluxed at 100 °C for 2 h. It should be mentioned that in order to remove the dissolved oxygen, the solution was deoxygenated with oxygen-free nitrogen for 30 min by bubbling nitrogen gas. During this reaction, chemically modified graphene oxide was partially reduced by hydrazine to PS grafted reduced graphene oxide, which in this paper is noted as PS-GO. The mixture was cooled to room temperature, and washed with *N, N*-dimethylformamide (DMF) and deionized water to remove the excess surfactants and residual monomer from the reaction mixture. This procedure was repeated more than three times. The purified product was kept in the DMF solution for the next step. For a comparison, partially reduced graphene oxide was also prepared with the same conditions, noted as rGO.

2.2.2 Fabrication of PA6/ABS/PS-GO Blend composites

The PA6/ABS/PS-GO blend composites were fabricated through a two-step procedure: solution blending of ABS with PS-GO, and subsequent melt compounding of PA6，ABS and the ABS/ PS-GO master batch. In the first step, ABS/PS-GO master batch with 5 wt% PS-GO was prepared via solution blending in DMF. The ABS/PS-GO mixture was kept stirring at 80 °C to remove partial DMF solvent, and then it was dried in vacuum oven at 60 °C for at least 24 h to make sure that all the residual DMF were removed and the weight of resultant black

solid kept constant. In the second stage, the obtained master batch, PA6 and ABS were melt-blended on a twin-screw extruder SHJ-20 (Nanjing Ruiya, China) at a screw speed of 150 rpm, and a temperature profile of 170, 190, 210, 230, 250, 250, 245°C from the feeding zone to die. The extrudate was water-cooled and chopped into pellets, and then dried in a vacuum oven for 24 h at 50 °C. These blends were then injection-molded to obtain the dumbbell specimens (with a width of 4.5 mm and a thickness of 2.0 mm) and the rectangular specimens (with a width of 10 mm and a thickness of 4.0 mm) using the Haake minilab injection-molding machine (HAAKE MiniJet, Germany) at the melt temperature of 240 °C with the injection pressure of 700 bar. In the blend composites, the weight ratio between PA6 and ABS was maintained at 50:50, and the content of PS-GO was varied from 0 to 1 wt%. The sample notation was defined as P5A5Gx, where x represented the content of PS-GO in the blend composites. For example, P5A5G0.5 represented that PS-GO content was 0.5 wt%. For comparison, the binary PA6/ABS (50/50 wt%) blend, which was named as P5A5, was also prepared through the completely same processing procedures as was done for the blend composites

2.3 Characterization

2.3.1 Transmission electron microscopy (TEM)

A small amount of PS-GO was dispersed in DMF with the help of sonication, and the solution was used for TEM to characterize the microstructure of PS-GO. The phase morphology of the blend was also characterized using a transmission electron microscope (TEM) JEM-2100F (JEOL, Japan) with operating voltage of 200 kV.

2.3.2 Fourier transforms infrared spectrometer (FT-IR)

The structural analysis was conducted using a Fourier transform infrared spectrometer (FT-IR, Nicolet 5700, USA). The FTIR spectra were recorded on a KBr pellet in a frequency range of 4000 cm^{-1} to 400 cm^{-1}.

2.3.3 Thermal gravimetric analysis (TGA)

The thermal gravimetric analysis was conducted on a Q5000 thermo-analyzer instrument (TA Instruments Inc., USA) from 30 °C to 600 °C in air atmosphere with a heating rate of 10 °C /min. Before testing, all the samples were carefully grinded to powders to ensure sufficient diffusion of heat.

2.3.4 Wide angle X-ray diffraction (WAXD)

The interlayer spacing of Graphene and PS-GO (dried powder samples) were measured using a wide angle X-ray diffraction (WAXD) X'pert PRO diffractometer (PANalytical, the Netherlands) with Ni-filtered Cu Kα radiation. The continuous scanning angle range used in this study was from 5° to 50° and the measurement was operated at 40 kV and 40 mA.

2.3.5 Raman Spectrometer

Raman spectrum of rGO and PS-GO were recorded on a Laser Confocal Raman Microspectroscopy (LabRAM HR 800 UV, HPRIBA JOBIN YVON) with 633 nm laser excitation.

2.3.6 Mechanical properties measurement

Tensile properties were measured on an injection-molded bar using a tensile testing machine AGS-J (SHIMADZU, Japan) according to ASTMD 638. The sample had a width of 4.5 mm and a thickness of 2.0 mm. During the measurement, the gauge distance was set at 45 mm and an across-head speed of 5 mm/min was used. For the unnotched Izod impact strength, it was measured using a rectangular sample with the width and thickness of 10 and 4.0 mm,

respectively. The measurement was conducted on a XC-22Z impact tester (Chengdu, China) according to ASTMD 256-04. The measurements were mainly carried out at room temperature (23±1 °C), and for each sample, the average value of mechanical properties reported was derived from the data of more than 5 specimens.

2.3.7 Scanning electron microscopy (SEM)

The phase morphologies and tensile-fractured surface morphologies of the blend composites were characterized using a scanning electron microscope (SEM) Fei Inspect (FEI, the Netherlands) with an accelerating voltage of 20 kV. Before characterization, all the samples were coated with a thin layer of gold. To observe the tensile-fractured surface, samples were directly observed by SEM. To observe the phase morphologies, samples were first cryogenically fractured in liquid nitrogen, and then the fractured surface was immersed into the tetrahydrofuran (THF) solution at 80 °C for 3 h to remove ABS phase. After that, the treated surface was carefully washed using alcohol and water with the aid of sonication, successively.

2.3.8 Dynamic mechanical analysis (DMA)

The dynamic mechanical properties were measured using a dynamic mechanical analysis (DMA) Q800 (TA Instrument, USA). The single cantilever mode was selected. A rectangular sample, which was directly cut from an injection-molded bar, was used and it had a length of 35 mm, a width of 10 mm and a thickness of 4 mm. The measurement was carried out from 30 °C to 180 °C at a heating rate of 3 °C/min and at a frequency of 1 Hz.

3. Results and Discussion

3.1 Preparation and characterization of PS-GO

In order to evaluate the grafting efficiency, TEM was applied to observe the morphology of PS-GO. The TEM images (Fig. 1a) of the PS-GO distinctly reveal that synthesized polystyrene with a width of several couples of nanometers are attached along the edges of the stacked nanosheets with thickness of several nanometers. The similar morphology can be found with a similar ellipsoidal structure in PS grafted graphene [25]. FTIR spectra analysis was performed to confirm the chemical components of the PS-GO. Fig. 1b illustrates the FTIR spectra of the rGO, and PS-GO. Both the two curves of the two samples exhibit characteristic peaks at 3500 cm^{-1}, 1650 cm^{-1} and 1100 cm^{-1}. The band at 3500 cm^{-1} is attributed to the presence of free or associated hydroxyl groups and the broad peak at 1100 cm^{-1} derives from the associated C-O stretching vibrations, both of which are from the adsorbed bound water or the unreduced hydroxyl groups on the rGO. The band located at 1650 cm^{-1} is assigned to the C=C stretching vibrations in carboxyl and skeleton. As for the PS-GO, the newly emerged peaks located at 1580,1490,1446,750,530 cm^{-1} correspond to absorptions of the benzene ring of PS segments, while the peak at 2922 cm^{-1} arises from the attachment of additional methylene groups. It is obviously seen from the FTIR spectra that the PS chains are attached on the rGO. It should be noted that during the preparation of PS-GO, the self-polymerized PS and residual monomer have been carefully washed and removed. Hence, all the characterization of PS-GO is for the grafted PS on rGO. The underlying mechanism for functionalization is derived from the in-situ emulsion polymerization and subsequent reduction of graphene oxide. During the emulsion polymerization, the surfactant micelles were firstly adsorbed onto the edge of graphene oxide nanosheets which were full of oxygen-containing groups; Styrene monomers were attached on the hydrophobic end of surfactant, and then initiator was applied to initiate the emulsion polymerization [19].

Fig.2 shows thermogravimetric curves from the rGO, polystyrene and PS-GO. As for polystyrene, the decomposition starts at 350 ^{o}C. The mass loss of rGO starts at 200 ^{o}C, which is attributed to the pyrolysis of oxygen-containing groups such as hydroxyl, carboxyl etc. The

PS-GO exhibits two characteristic mass losses, one appears at 200 $^{\circ}$C and the other one starts

at 350 $^{\circ}$C, corresponding to the pyrolysis of oxygen-containing groups and decomposition of

PS, respectively. Combining with FTIR, TGA and TEM results, it is obviously found that PS

is successfully grafted onto the surface of graphene sheets; although a small amount of

oxygen containing groups are still attached on the graphene surface. It should be noted that

reduction could not completely remove the polar groups, hence a small amount of oxygen

containing groups are still unremoved.

Raman spectroscopy is a powerful tool for describing the carbonaceous materials with

chemical functionalization or physical wrapping via distinguishing ordered and disordered

crystal structures of carbon. Fig. 3 shows the Raman spectra of rGO and PS-GO to evaluate

the structures of rGO before and after functionalization. The main features of graphene in the

Raman spectra are G peak at 1591 cm^{-1} and D peak at 1336 cm^{-1}. The G peak originates from

the in-plane vibration of sp^{2} carbon atoms while the D peak is assigned to the some structure

defects such as localized sp^{3} carbon atoms from oxygen containing functional groups,

vacancies and topological defects, which may benefit the chemical grafting of polymers to

graphene nanosheets. It can be observed that the two curves for rGO and PS-GO are similar

in terms of the shapes and positions of G and D peaks. It is necessary to note that the peak

intensity ratios I (D)/I (G) of rGO and PS-GO are 1.25 and 1.18, respectively. This result can

also be explained if new graphitic domains are created that are higher in number after grafting

for PS-GO [26]. Such disorders and defects are also reflected in the red-shifted D peak (such

as from 1336 cm^{-1}to 1333 cm^{-1}in PS-GO) and the red-shifted (such as from 1591 cm^{-1} to

1584 cm^{-1} in PS-GO) of PS-GO compared with rGO. According to Rao[27],the G band

position varies from sample to sample because of the difference in the number of layers, so

the red-shifted G peak may be attributed to that the G-band position decreases with an

increasing number of layers in their solid states[28]. The red-shifted D peak may be

associated with PS chains chemically bonding to rGO. On the other hand, the substantial

structure of the carbon network in rGO and PS-GO has been maintained after PS grafting onto the edge of graphene nanosheets.

For a further confirmation, the XRD patterns of rGO and PS-GO were recorded in Fig. 4. The (002) diffraction peak of rGO is assigned at about 24°, and the interlayer spacing is about 0.37 nm. Concerning about the PS-GO, the (002) diffraction peak is moved forward to 21.4^o with corresponding spacing of 0.41 nm. The XRD results illustrate that attachment of PS onto the edge of PS-GO nanosheets can disturb the Vander Waals interaction of stacked PS-GO layers, exfoliate the PS-GO layers and furthermore enlarge the spacing of the nanosheets. Combined with the results shown above, it should be mentioned that some oxygen-containing groups for PS-GO are still unremoved as shown above. Hence, the GO sheets were partially reduced in order that the amounts of oxygen containing groups were lowered and the strong polarity of GO was avoided. In this case, the PS-GO show "amphiphilic" characteristic features, which means unremoved oxygen containing groups exhibit the possibility to interact with polar polymers or polymers containing some functional groups [29] while the grafted PS would like to entangle with polymers containing benzene rings or carbon structures via intermolecular interaction, which could be an important driving force to tailor the morphology of immiscible blends, especially for the compatibilization of immiscible blends. Based on these predictions, polymer blend comprised of polar polymer PA6 and ABS containing PS segments was chosen as our research target. Importantly, PA6/ABS is of great potential in industrial and commercial fields, therefore, investigations on the effects of PS-GO on PA6/ABS is of great significance.

3.2 Mechanical property of ternary composites

The elongation at break is an important factor to directly judge toughness of polymer blends. The strain-stress curves sheds light on the load vs. deformation features of the blend

composites. Fig. 5a displays the representative strain-stress behaviors of the various blended composites. It can be found that PA6/ABS with and without PS-GO exhibit similar deformation behavior containing elastic deformation, yielding and fracture. Elongation at break of the blend without PS-GO is only 11%; while it is evident from Fig. 5a that addition of PS-GO has increased the ductility. When 0.3 and 0.5 wt% PS-GO were incorporated into blends, the elongation at break increased to 25% and 42% respectively indicating that these blends have a greatly improved ductility. However, a decrease of elongation at break can be found possibly due to the aggregation of 1 wt% PS-GO. For a clear illustration, the tensile strength, modulus and elongation at break of samples with PS-GO are respectively shown in Fig. 5b. As for blend composites with PS-GO, great improvement on elongation at break can be achieved without any loss of tensile strength and modulus. Even the tensile strength and modulus exhibit slight increase which should be attributed to the reinforcing effect of PS-GO. On the other hand, seen from Fig. 5c, it is found that with increasing the concentration of PS-GO, the impact strength increases from 9.0 kJ/m^2 to 21 kJ/m^2 when 0.5 wt% PS-GO are incorporated into polymer blends. Similar to the elongation at break, when 1 wt% PS-GO are incorporated into polymer blends, aggregates of PS-GO cause the decrease of impact strength. The increase on impact strength reveals the presence of PS-GO in immiscible blend PA6/ABS is also benefit for the energy adsorption during impact strength, and a further study concerning about effects of PS-GO on the crack growth during the impact testing are needed in a future work.

As described above, the common toughening methods for the immiscible blend PA6/ABS reported in the literatures are mainly related to the addition of copolymer of other component，such as carbon nanotubes (CNTs). To better understand the toughening effect of PS-GO in the immiscible PA6/ABS blend, a comparison between our results and other results reported in the literatures are carried out as shown in Fig. 6, in which CNT, EMA-GMA

(ethylene methyl acrylate-glycidyl methacrylate), and EnBACO-MAH(ethylene-*n* butyl

acrylate-carbon monoxide-maleic anhydride) were utilized to modify PA6/ABS blends to

improve the interfacial adhesion and achieve the desired improvement on mechanical

properties[30, 31]. Among all these fillers or components, it is clearly seen that our PS-GO

exhibits the most effective toughening on PA6/ABS blends; in contrast, CNTs, EMA-GMA

and EnBACO-MAH did not show any positive role on the improvement of toughness. It is

clear that great improvement on fracture toughness and ductility is obtained by PS-GO, the

underlying mechanism needs to be clarified.

3.3 Toughening Mechanism

Morphology of polymer blends is one of the decisive factors that influence the final

properties. Fig. 7 shows the morphologies of PA6/ABS blends with different contents of PS-

GO. For a clear observation, the ABS component was removed using chemically etching of

THF; therefore, the dark domain corresponds to the removed ABS and the gray domain is the

PA6. All the samples indicate that ABS phase disperse in the PA6 matrix. It should be noted

that the weight ratio of PA6 and ABS is 50:50, and the morphology of PA6/ABS is in the

intermediate state between sea-island and co-continuous structure. Seen from Fig. 7, more

elongated or connected ABS domain could be differentiated in polymer blend composites

with increasing the content of PS-GO, although no significant change on phase morphology

can be observed. The continuity of PA6 domain, calculated by Image J1.47n software [32],

which was used to transform the SEM images with the same magnification into numerical

values, exhibits a gradual increase with increasing the content of PS-GO as show in Fig. 8. As

for the PA6/ABS blends, the gray domain with the continuity of 69% can be found. The

continuity of PA6 is gradually increased to 76.2%, 75.0% and 86.7% when 0.3, 0.5, 1.0 wt%

PS-GO are present in the blend composites, respectively. The increasing trend for the

continuity of PA6 could be observed with increasing the content of PS-GO. The increased

continuity exhibits morphology coarsening and indicates the decreased interfacial areas which enables elongated phase to share more in the load bearing capability, suggesting that increased continuity is more effective for lowering interfacial tension [33, 34]. Based on these observations and analysis, the continuity induced by PS-GO plays a positive role on the improvement of toughness. However, when 0.5wt% PS-GO were incorporated into polymer blends, the toughness including both elongation at break and compact strength exhibit greatest increase while the continuity shows only slight increase. It is clear the phase morphology is not the key to the improvement of toughness.

In order to further explore the toughness mechanism of PS-GO in PA6/ABS, the tensile-fractured surfaces along the tensile direction were observed by SEM and the results are shown in Fig. 9. As shown in Fig. 9(a), the blank PA6/ABS blend exhibits the typical layered fibrillation structure due to the severe plastic deformation of matrix during the tensile test. It can be observed that some dispersed ABS particles have been pulled out from the matrix, as shown in inset of Fig. 9(a), indicating the weak interfacial adhesion between PA6 and ABS. As for the blend with PS-GO, the similar morphology with fibrillation structure could be observed. However, the ABS particles disappeared and only the deformed fibrils of ABS and PA6 could be found, finer morphology without severe detaching is observed in PA6/ABS blend with PS-GO. These observations indicate the interfacial adhesion between PA6 and ABS is identified by PS-GO.

To clarify this observation, the relaxation behaviors of all samples were investigated by DMA to evaluate the chain mobility of PA6 and ABS with incorporation of PS-GO. Fig.10 shows the loss factor (tan δ) for PA6/ABS blend and their blend composites with PS-GO. The loss factor peak at temperature of 30 $^{\circ}$C is assigned to the glass transition of PA6 chain segments; the loss factor peak at higher temperature of 116.5 $^{\circ}$C is for the glass transition of PS chain segments of ABS. It should be found that T_g of ABS shifts to lower temperature

gradually with increasing the contents of PS-GO, which indicates that the glass transition

behaviors of ABS component are influenced by PS-GO. This confirms that the ABS chains

diffuse or dissolve in Nylon 6 domain when PS-GO is incorporated in immiscible blends, as

demonstrated in polyvinylidene fluoride (PVDF)/PA6/GO ternary composites [35]. On the

other hand, the T_g of PA6 exhibits little change with incorporation of PS-GO. The different T_g

variation trend of PA6 and ABS illustrates the possibility of PS-GO locating at interface of

PA6 and ABS, furthermore promoting the interfacial adhesion.

   In order to verify the localization of PS-GO at interface, the interfaces of the immiscible

PA6/ABS blends with and without PS-GO have been carefully observed as shown in Fig. 11,

the interfaces for the blends with PS-GO (Fig. 11b) are coarser compared with that of the

blank PA6/ABS blend (Fig. 11a) and some folds of sheets-like structure can be found as

shown by arrows. On the other hand, it should be noted that the PS-GO with two dimensional

planes exhibits high interfacial stability, allowing it to more readily cover the interface [36].

Therefore it is reasonably proposed that PS-GO is located at interface, leading to the polymer

chain diffusion crossing the interface and variation of T_g of ABS.

   According to the previous observation, the toughening mechanism of PS-GO in the

immiscible PA6/ABS blend can be further understood as shown in the schematic picture in

Fig. 12. Phase separation with clear interface can be found in neat PA6/ABS blend due to the

unfavorable interaction between PA6 and ABS. With the introduction of PS-GO, these

nanosheets functionalized PS chains can adsorb some PS section of ABS on their basal planes

due to the $\pi-\pi$ interaction between PS section in ABS and PS chains grafted on GO[37]. On

the other hand, the unremoved groups containing oxygen on GO basal planes have strong

interaction with PA6 which is originated from the hydrogen bonding between amide group of

PA6 and the hydroxyl on rGO [38]. On the other hand, as we know, the fillers in immiscible

blends would like to migrate to component with lower viscosity or better interaction with

filler. In this case, PS-GO are inclined to migrate from ABS/PS-GO masterbatch to the PA6 due to the lower viscosity of PA6 and the hydrogen bonding between PS-GO and PA6. As we know, due to the $\pi-\pi$ interaction between PS section in ABS and PS chains grafted on GO, partial ABS are adsorbed on PS-GO in ABS/PS-GO masterbatch. When ABS/PS-GO blended with PA6, PS-GO would like to migrate from ABS to PA6 with lower viscosity. In this case, partial ABS adsorbed on PS-GO could solve or diffuse into PA6 domain as accompanied with the migration of PS-GO from ABS to PA6; and the phase coarsening may be allowed. It is worthy to be noted that partial PS-GO may migrate to the interface and weave across the interface, realizing the formation of entanglements and reducing unfavorable contacts between PA6 and ABS as shown in Fig.12. In this case, the interfacial adhesion was intensified, leading to the great improvement of ductility. On the other hand, in a viewpoint of intrinsic structure of graphene, the wrinkles on PS-GO can enhance the interfacial adhesion between polymer and PS-GO; and the deflection of crack induced by graphene may also play a positive role on toughening which needs a further discussion in future needs work. [9, 10, 11]

4. Conclusion

In summary, we chemically tailored the structure of rGO via grafting PS chains onto the rGO. With the incorporation of PS-GO into the immiscible PA6/ABS blend, both the tensile ductility and impact strength of the blend composites are greatly enhanced, indicating the toughening effect of PS-GO. Further studies on the morphology demonstrated that the addition of PS-GO slightly increase the continuity of ABS phase, obviously it is not the key to the great improvement on ductility. DMA, SEM observation results reveal the underlying mechanism for the toughening, which is believed to be the enhanced interfacial adhesion between ABS and PA6 with the presence of PS-GO locating at interface. Furthermore, the intensified interfacial adhesion could be attributed to the dual effects of PS-GO with two

components, in which one is the the π−π interaction between PS section in ABS and PS

chains grafted on PS-GO，and the other is the hydrogen bonding between PS-GO and PA6.

Acknowledgement

Reference

[1]L. A. Utracki, *Polymer Alloys and Blends*, Hanser Publishers, New York, 1990.

[2]K. Joseph, S. Varghese, G. Kalaprasad, S. Thomas, L. Prasannakumari, P. Koshy and C. Pavithran, *Eur. Polym. J*, 1996, **32**, 1243.

[3]S. Y. Fu, X. Q. Feng, B. Lauke and Y. W. Mai, *Compos. Part B- Eng*, 2008, **39**, 933.

[4]D. R. Paul and C. B. Bucknall, *Polymer Blends: Formulation and Performance*, John Wiley & Sons, New York, 2000.

[5]S. C. Tjong and T. C. Ke, *Eur. Polym. J*, 1998, **34**, 1565.

[6]H. Tanaka, A. J. Lovinger and D. D. Davis, *Phys. Rev. Lett*, 1994,**72**, 2581.

[7]J. S. Hong, H. Namkung, K. H. Ahn, S. J. Lee and C. Kim, *Polymer*, 2006, **47**, 3967.

[8]L. Elias, F. Fenouillot, J. C. Majeste and P. Cassagnau, *Polymer*, 2008, **49**, 4378.

[9]A. K. Geim and K. S. Novoselov, *Nat. Mater*, 2007, **6**, 183.

[10]H. Kim, A. A. Abdala and C.W. Macosko, *Macromolecules*, 2010, **43**, 6515.

[11]S. Stankovich, D. A. Dikin, G. H. B. Dommett, K. M. Kohlhaas, E. J. Zimney, E. A. Stach, R. D. Piner, S. T. Nguyen and R. S. Ruoff, *Nature*, 2006, **442**, 282.

[12]M. A. Rafiee, J. Rafiee, I. Srivastava, Z. Wang, H. Song, Z. Z. Yu and N. Koratkar, *Small*, 2010, **6**, 179.

[13]H. He, J. Klinowski and M. Forster, *Chem. Phys. Lett*, 1998, **287**, 53.

[14]S. Stankovich, R. Piner, X. Chen, N. Wu, S. Nguyen and R. Ruoff, *J. Mater. Chem*, 2006, **16**, 155.

[15]Y. W. Cao, J. Zhang, J. C. Feng and P. Y. Wu, *ACS Nano*, 2011, **5**,5920.

[16]Y. Cao, J. Feng and P. Wu, *J. Mater. Chem*, 2012, **22**, 14997.

[17]Y. Tan, L. Fang, J. Xiao, Y. Song and Q. Zheng, *Polym. Chem.UK*, 2013, **4**, 2939.

[18]W. H. Liao, S. Y. Yang, J. Y. Wang, H. W. Tien, S. T. Hsiao, Y. S. Wang and Y. F. Wu, *ACS Appl. Mater. Inter*, 2013, **5**, 869.

[19]H. Hu, X. Wang, J. Wang, L. Wan, F. Liu, H. Zheng and C. Xu, *Chem. Phys. Lett*, 2010, **484**, 247.

[20]S. Sun, Y. Cao, J. Feng, and P. Wu, *J. Mater. Chem*, 2010, **20**, 5605.

[21]M. Fang, K. Wang, H. Lu, Y. Yang and S. Nutt, *J. Mater. Chem*, 2010, **20**, 1982.

[22]E. Tkalya, M. Ghislandi, A. Alekseev, C. Koning and J. Loos, *J. Mater. Chem*, 2010, **20**, 3035.

[23]C. Tang, G. Long, X. Hu, K. Wong, W. Lau, M. Fan, J. Mei, T. Xu, B. Wang and D. Hui, *Nanoscale*, 2014, **6**, 7877.

[24]W.S. Hummers and R.E. Offeman, *J. Am.Chem. Soc*, 1958, **80**, 1339.

[25]Y. T. Liu, J. M. Yang, X.M. Xie and X. Y. Ye, *Mater. Chem. Phys*, 2011, **130**, 794.

[26]S. Stankovich, D. A. Dikin, R. D. Piner, K. A. Kohlhaas, A. Kleinhammes, Y. Jia and R. S. Ruoff, *Carbon*, 2007,**45**, 1558.

[27]C. Rao, K. Biswas, K. Subrahmanyam and A. Govindaraj, *J. Mater. Chem*, 2009, **19**, 2457.

[28]J. Shen, Y. Hu, M. Shi, X. Lu, C. Qin, C. Li and M. Ye, *Chem. Mater*, 2009, **21**, 3514.

[29]R. Rafiq, D. Cai, J. Jin and M. Song, *Carbon*, 2010, **48**, 4309.

[30]X. Q. Liu, W. Yang, B. H. Xie and M. B. Yang, *Mater. Design*, 2012, **34**, 355.

[31]G. Ozkoc, G. Bayram and E. Bayramli, *J.Appl. Polym. Sci*, 2007, **104**, 926.

[32]M. Liebscher, M. O. Blais, P. Pötschke and G. Heinrich, *Polymer*, 2013, **54**, 5875.

[33]R. C. Willemse, A. P. De Boer, J. Van Dam and A. D. Gotsis, *Polymer*, 1998,**39**, 5879.

[34]J. Li, P. L. Ma and B. D. Favis, *Macromolecules*, 2002, **35**, 2005.

[35] J. Yang, C. Feng, J. Dai, N. Zhang, T. Huang and Y. Wang, *Polym. Int*, 2013, **62**, 1085.

[36]A. Göldel, A. Marmur, G. R. Kasaliwal, P. Pötschke and G. Heinrich, *Macromolecules*, 2011, **44**,6094.

[37]M. Yang, V. Koutsos and M. Zaiser, *J. Am Chem. B*, 2005, **109**, 10009.

[38]X. Zhang, X. Fan, H. Li, and C. Yan, *J. Mater. Chem*, 2012,**22**, 24081.
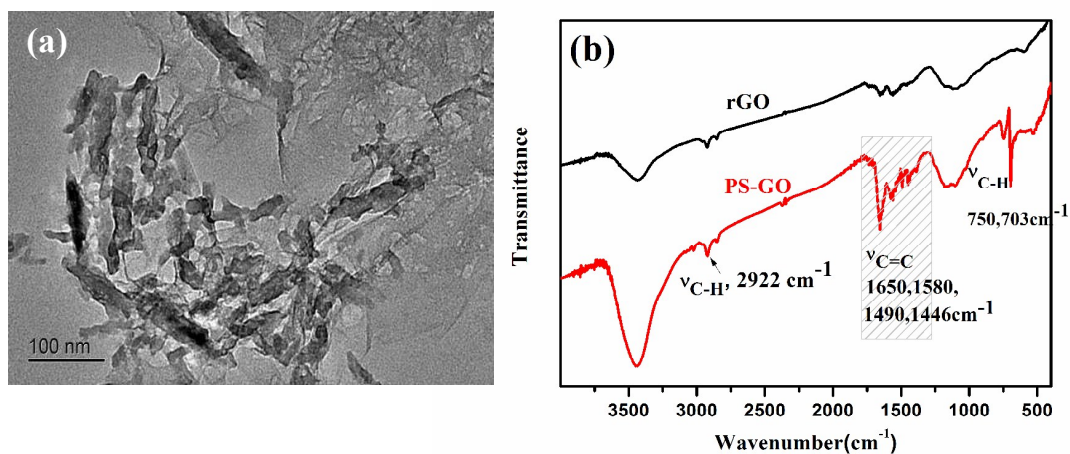
Fig.1 (a) TEM photo of PS-GO; (b) FTIR spectra of rGO and PS-GO.
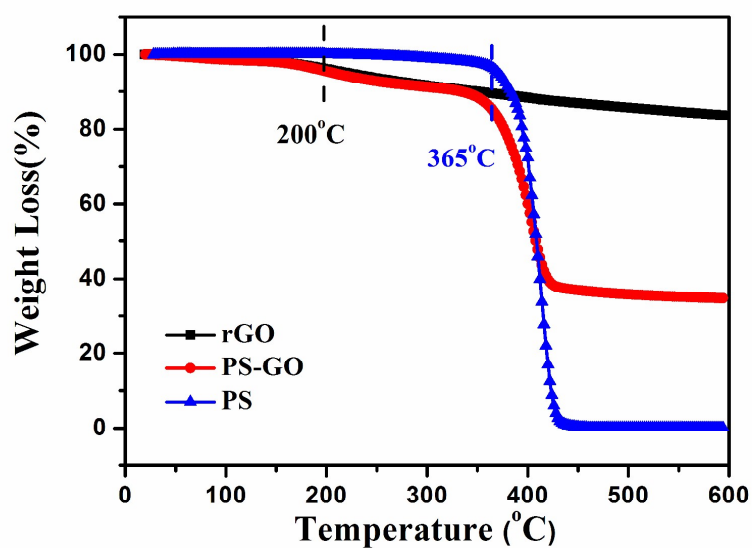
Fig.2 TGA curves of the rGO, PS and PS-GO.
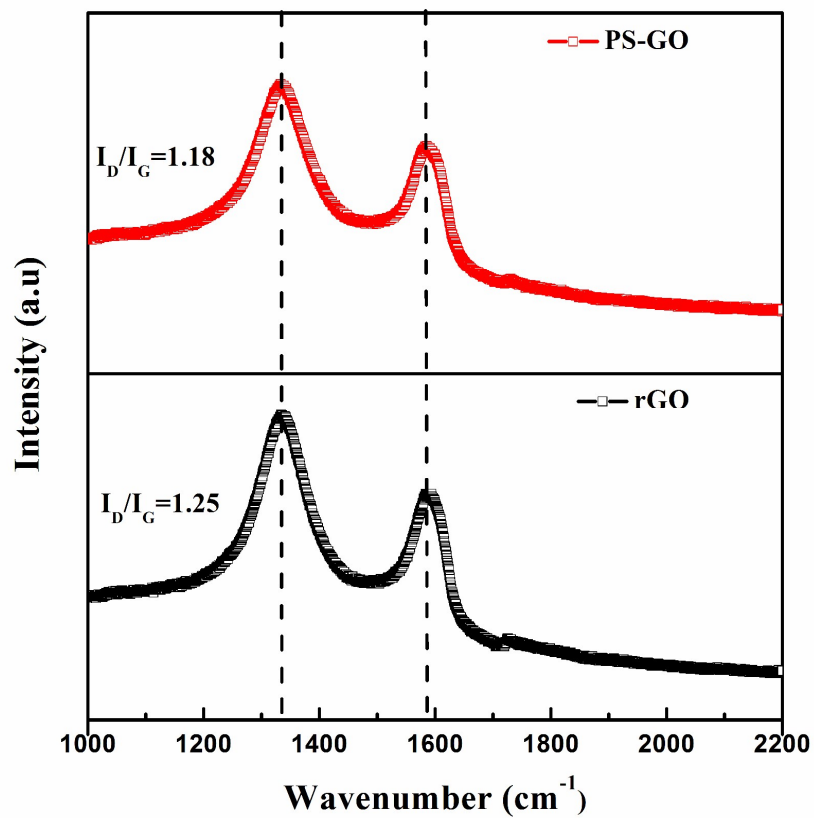
Fig.3 Raman spectra of rGO and PS-GO.
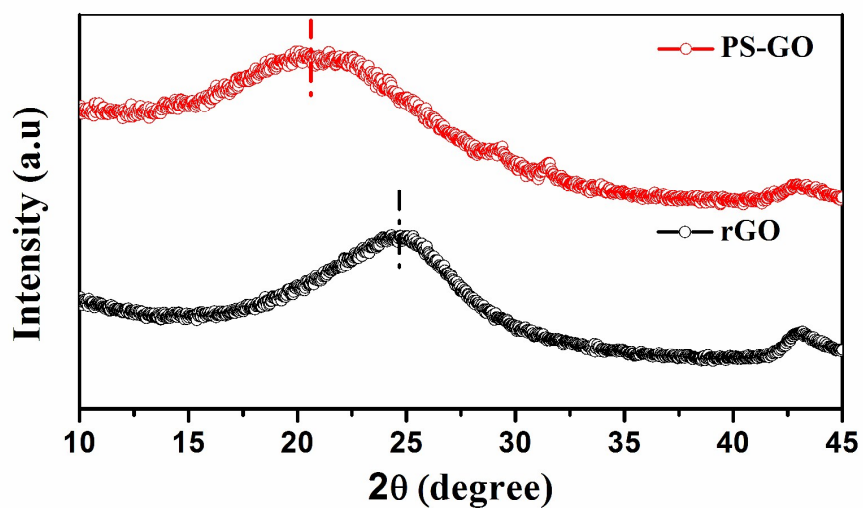
Fig.4 XRD spectra of rGO and PS-GO.
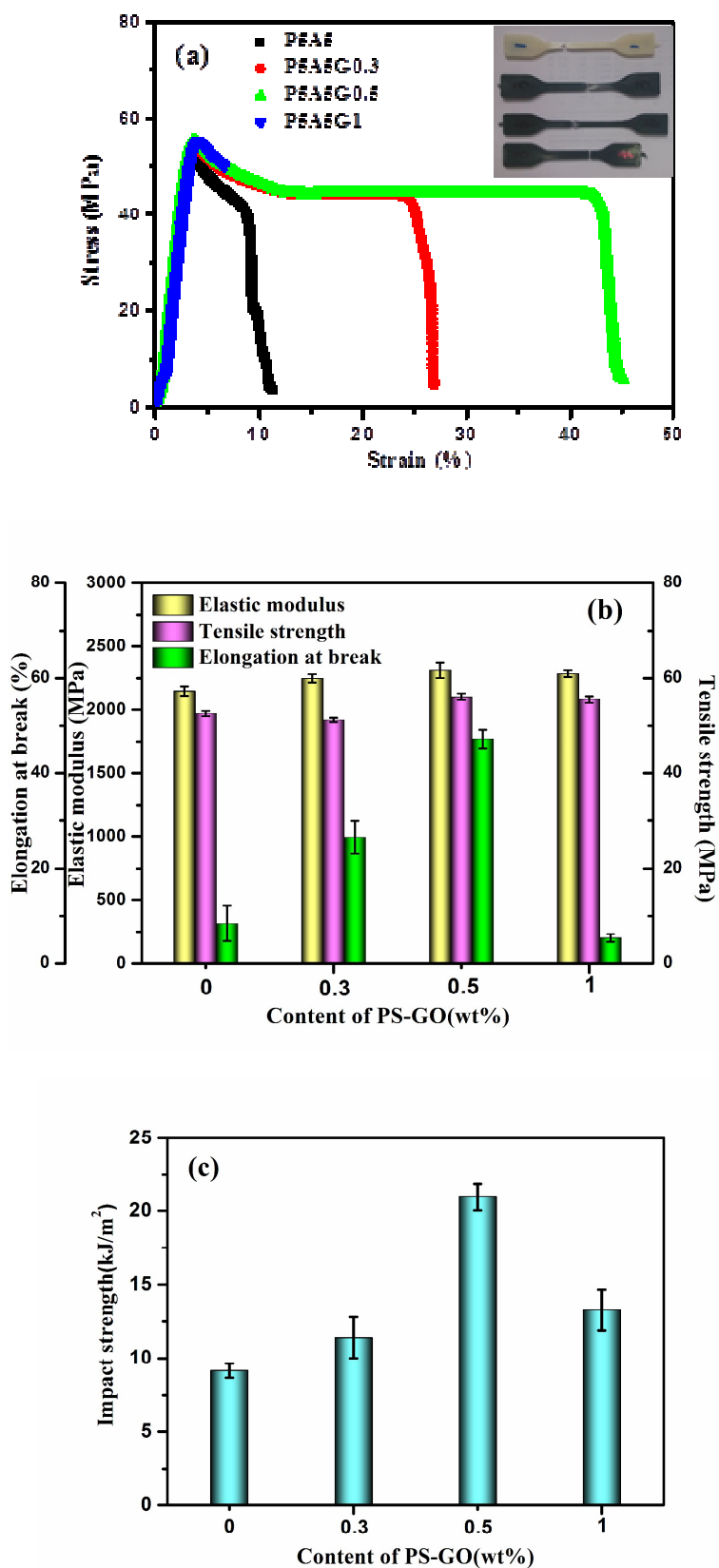
Fig.5 (a) Typical strain-stress curves of samples and (b) the corresponding tensile properties; (c)

Variation of Impact strength of PA6/ABS/PS-GO blend composites *versus* PS-GO content.
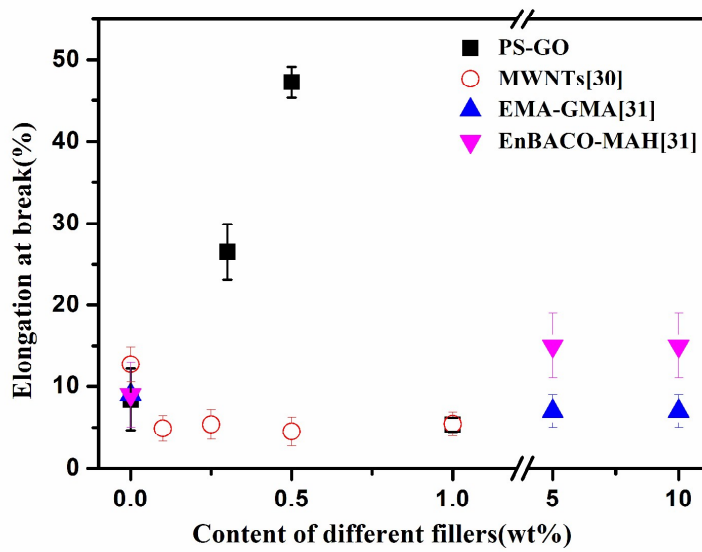
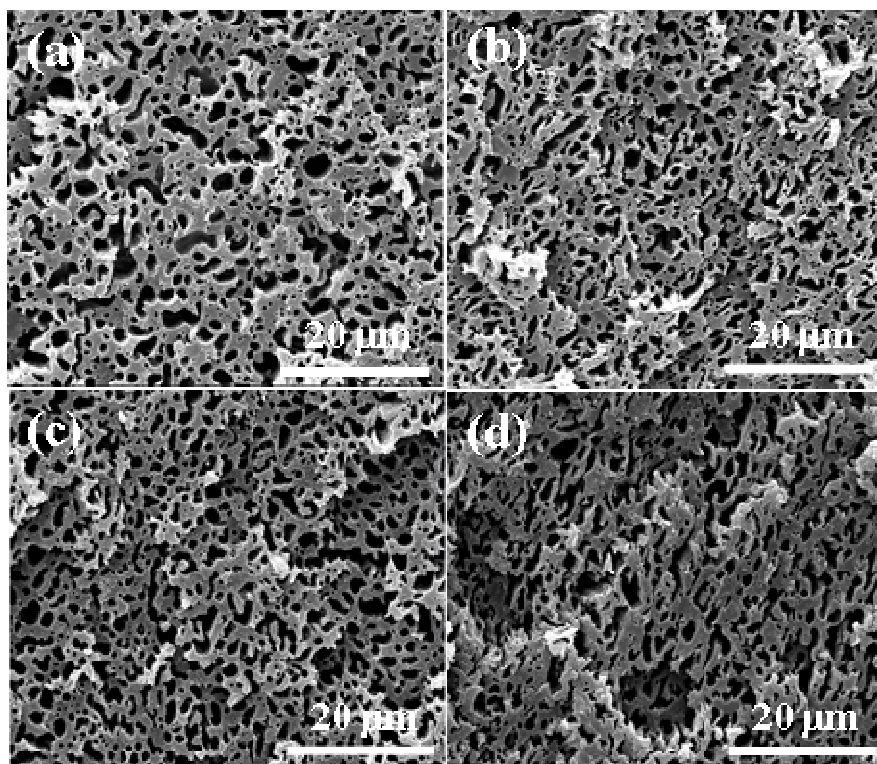Fig.6 Elongation at break of PA6/ABS with the addition of different fillers for comparison.

Fig.7 SEM photos of PA6/ABS/PS-GO blend composites with different contents. (a) 0 wt%; (b)0.3

wt%; (c) 0.5 wt%; (d) 1 wt%.
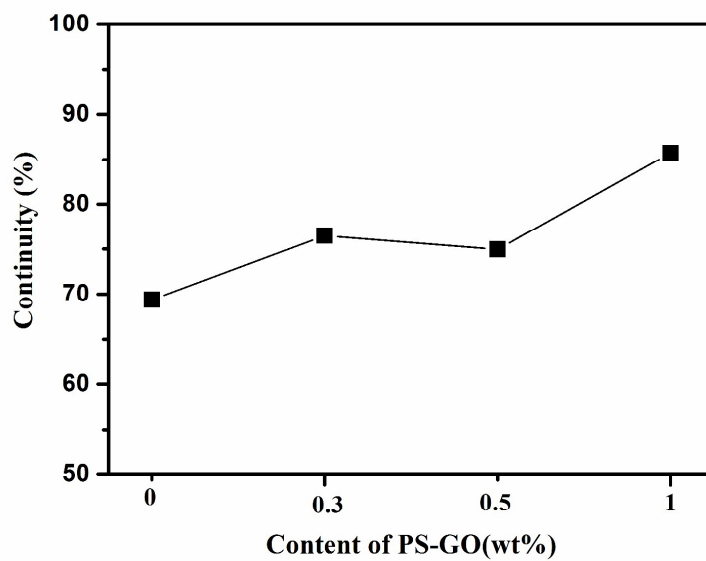
Fig. 8 Continuity of PA6 in PA6/ABS blends with different contents of PS-GO.
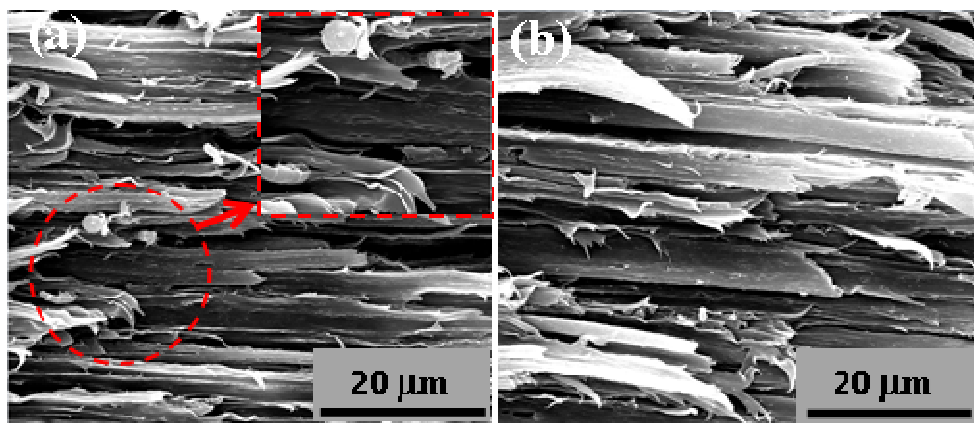
Fig. 9 SEM images showing the tensile-fractured surface morphologies of (a) PA6/ABS blend and (b)
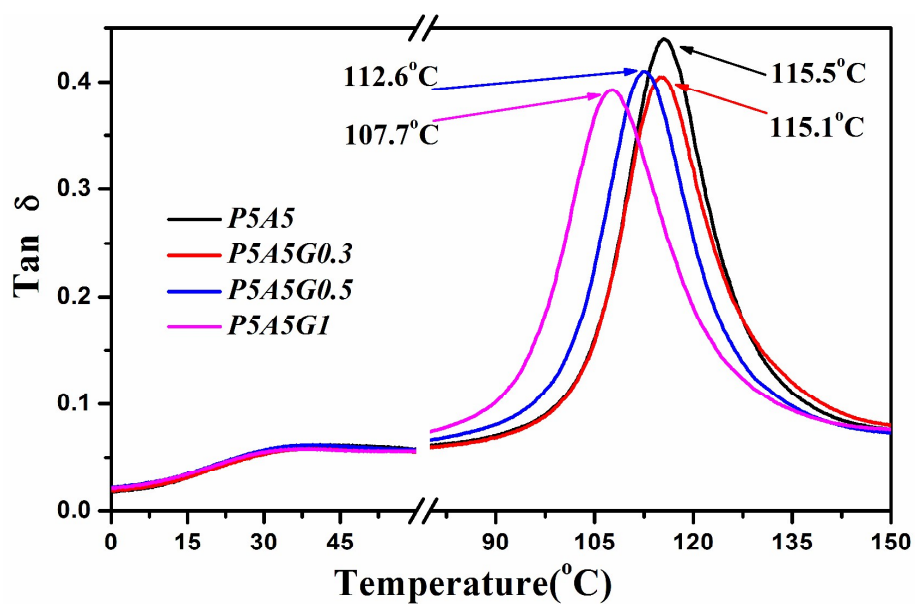
PA6/ABS/PS-GO blend composites with 0.5wt% PS-GO.

Fig. 10 Loss factor of the PA6/ABS blend and the PA6/ABS/PS-GO blend composites obtained
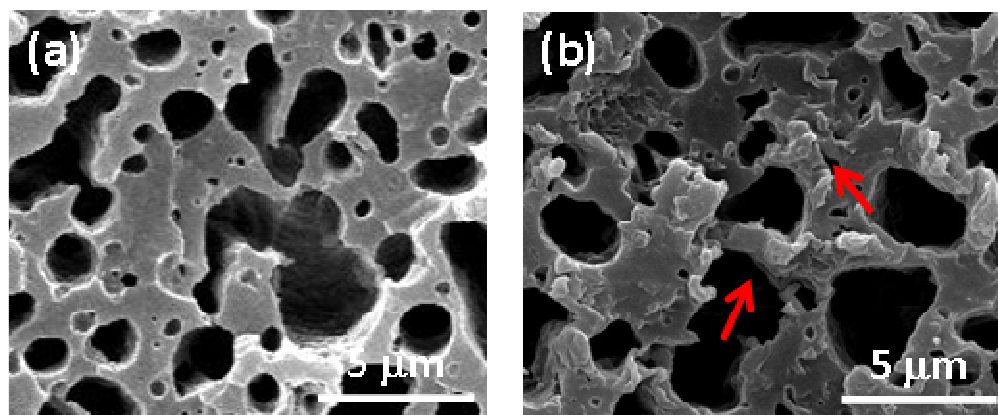
through DMA measurements.

Fig. 11 Interface of (a) PA6/ABS blend and (b) PA6/ABS/PS-GO blend composite
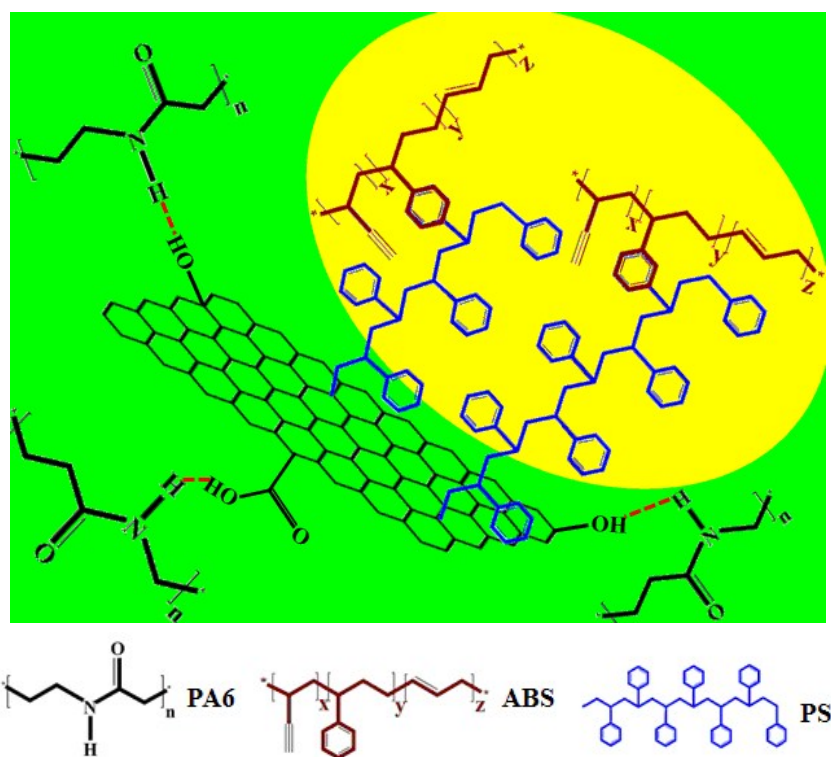
with 0.5 wt% PS-GO.

Fig. 12 Schematic showing of dual effects of PS-GO with PA6 and ABS components.

Largely enhanced fracture toughness of an immiscible polyamide 6/acrylonitrile-butadiene-styrene blend achieved by adding chemically modified graphene oxide

Wenbin Huang, Tingting Zhang, Jinghui Yang*, Nan Zhang, Ting Huang, Yong Wang*

Key Laboratory of Advanced Technologies of Materials (Ministry of Education), School of Materials Science and Engineering, Southwest Jiaotong Universtiy, Erhuan Road, North I, No 111, Chengdu, Sichuan 610031, China
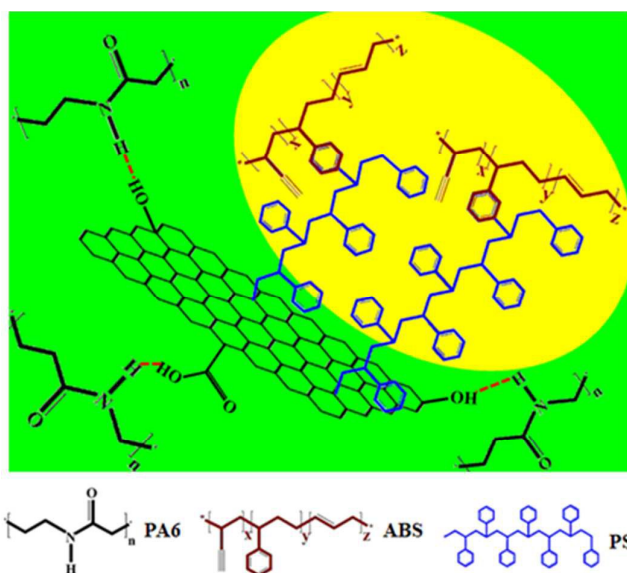
Schematic showing of dual effect of PS-GO with PA6 and ABS components.